PLANAR RRRP MECHANISM DESIGN PARAMETER SPACE

Alia Nichol, Mirja Rotzoll, M. John D. Hayes

Department of Mechanical and Aerospace Engineering, Carleton University, Ottawa, ON K1S 5B6, Canada
Email: alia.nichol@carleton.ca; mirja.rotzoll@carleton.ca; john.hayes@carleton.ca

ABSTRACT

A complete classification scheme of the mobility characteristics of the input link for every planar RRRP linkage reported in this paper is obtained in a novel and efficient way. To lay the foundation of this work, recent results are first briefly summarised. The algebraic input-output (IO) equation for any planar RRRP linkage is obtained by simply re-collecting the coefficients in the algebraic IO equation for a general planar 4R linkage in terms of the input link angle and the output slider linear displacement. The coefficients factor to two pairs of bilinear terms in the design parameters, the lengths of the input and coupler links and the offset distance of the slider longitudinal centreline from the ground-fixed R-pair centre. These four bilinear factors can be viewed as the four faces of a regular square pyramid in the three-dimensional space implied by the three design parameter directed distances. Intersections of the pyramid with a plane represented by any non-zero value of the offset distance produce line bound regions each containing points that represent all possible planar RRRP linkages. The numerical values of two of the bilinear factors of the algebraic IO equation imply a complete classification scheme for the mobility characteristics of the input links of these planar four-bar mechanisms based on the critical input angles (if they exist) and the extreme P-pair travel.

Keywords: planar RRRP linkages; kinematic synthesis; double points of planar algebraic equations; design parameter space; input link mobility classification.

L'ESPACE DES PARAMÈTRE DE CONCEPTION POUR LES MÉCANISMES PLANAIRES RRRP

RÉSUMÉ

Cet article présente un système obtenu de manière novatrice et efficace permettant une classification complète des caractéristiques de mobilité d'un lien d'entrée pour chaque méchanisme RRRP planaire. Pour jeter les bases de ce travail, les résultats récents sont d'abord brièvement résumés. L'équation algébrique entrée-sortie (IO) pour toutes méchanismes RRRP planaires est obtenue en recueillant simplement les coefficients dans l'équation algébrique IO pour une méchanisme planaire 4R et en les exprimant en fonction de l'angle d'entrée et du déplacement de la liaison glissière de sortie. Ces coefficients se factorisent en deux paires de termes bilinéaires dans les paramètres de conception. Ces paramètres étant : les longueurs du lien d'entrée et de la bielle ainsi que la distance séparant l'axe longitudinal de la liaison glissière du centre de la paire R fixée au sol. Ces quatre facteurs bilinéaires peuvent être interprétés comme les quatre faces d'une pyramide à base carrée dans l'espace tridimensionnel défini par les trois distances des paramètres de conception. Les projections de la pyramide sur un plan d'une valeur positive quelconque parmi les distances de decalage de l'axe de la liaison glissière produisent des régions liées contenant chacune les points qui représentent toutes les méchanismes planaires RRRP possibles. Des valeurs numériques de deux des facteurs bilinéaires de l'équation algébrique IO découlent un système de classification complet des caractéristiques de mobilité des liens d'entrée pour ces mécanismes planaires à quatre barres défini par les angles d'entrée critiques et la course extreme de la liaision prismatique.

Mots-clés : méchanismes RRRP planaires ; synthèse cinématique ; points doubles des equations planaires ; espace des paramètres de conception ; classification de mobilité de la pièce d'entrée.

1. INTRODUCTION

The planar RRRP four-bar linkage, colloquially known as the crank-slider, has been the literal workhorse in the realm of mechanical and aerospace engineering for centuries, if not millennia [1, 2]. While the trigonometric analytical methods to study the relationship between the motions of the input and output links based on the distances between the R-pair centres as well as the offset and inclination angle of the P-pair have existed for at least 150 years [1], purely algebraic methods have not. Recent work by Rotzoll et al. [3, 4] has yielded the remarkable result that the very same algebraic input-output (IO) equation for planar 4R linkages, an algebraic polynomial in terms of the tangent half-angle parameters of the input and output link angles with coefficients comprised of linkage design parameters, has the IO equations for planar four-bar linkages that contain one or two P-pairs embedded in it. That is, one need only collect the planar 4R algebraic IO equation in terms of the input and output parameters for RRRP or PRRP planar linkages. The new insight into the structure of the IO equations yielded by this is sufficient justification to warrant further investigation in this area.
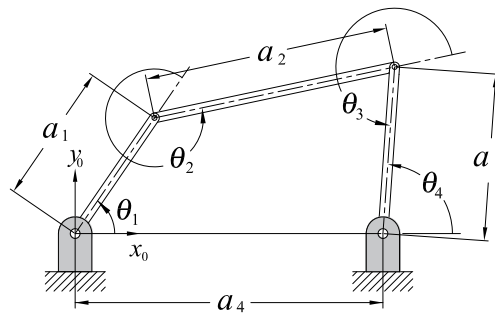

Fig. 1. Planar 4R closed kinematic chain.

The general IO equations for the RRRP and PRRP linkages and their inversions are naturally embedded in that of the planar 4R. The algebraic IO equation of an arbitrary planar 4R linkage illustrated in Fig. 1 is represented as

$$Av_1^2 v_4^2 + Bv_1^2 + Cv_4^2 - 8a_1 a_3 v_1 v_4 + D = 0, \tag{1}$$

where

$$
\begin{aligned}
A &= (a_1 - a_2 - a_3 + a_4)(a_1 + a_2 - a_3 + a_4) = A_1 A_2; \\
B &= (a_1 - a_2 + a_3 + a_4)(a_1 + a_2 + a_3 + a_4) = B_1 B_2; \\
C &= (a_1 - a_2 + a_3 - a_4)(a_1 + a_2 + a_3 - a_4) = C_1 C_2; \\
D &= (a_1 + a_2 - a_3 - a_4)(a_1 - a_2 - a_3 - a_4) = D_1 D_2; \\
v_1 &= \tan\left(\frac{\theta_1}{2}\right); \quad v_4 = \tan\left(\frac{\theta_4}{2}\right).
\end{aligned}
$$

The joint angle parameters v_1 and v_4 represent the tangent half-angles of linkage input and output angles, θ_1 and θ_4. The eight bilinear factors of the coefficients A, B, C, and D in Eq. (1) depend on the signed numerical values of the four a_i link lengths. In this formulation the input link parameter, a_1, is always positive but the remaining three a_i directed distances are the unique eight permutations of positive and negative signs in each factor. Hence, the eight bilinear factors represent eight distinct planes. Treating the a_i as mutually orthogonal basis directions in the hyperplane $a_4 = 1$ the eight planes intersect in the only uniform polyhedral compound [5], called the stellated octahedron, which has order 48 octahedral symmetry:

a regular double tetrahedron that intersects itself in a regular octahedron [6]. The location of a point in this space completely determines the mobility of the input and output links and hence it is termed the *design parameter space* of planar 4R linkages.

The R-pair axes of a spherical 4R mechanism all intersect at the centre of the sphere, see Fig. 2b. Those of a planar 4R mechanism are all parallel; they can be thought of as intersecting in a common point at infinity of the projective extension of the Euclidean plane of the planar 4R. As shown in [4, 7], this means that the planar 4R mechanism is a special case of the spherical 4R. In the limit, as the radius of the sphere tends towards infinity, the algebraic IO equations of the spherical and planar 4R mechanisms are projectively equivalent. The work presented in [5] reveals that the design parameter space of spherical linkages comprises eight cubic surfaces which intersect the design parameter space of planar 4R linkages in 12 real lines, the edge lines of the stellated octahedron, see Fig. 2a. Earlier work by Gosselin and Angeles [8, 9] in the late 1980's examined the spaces formed by the Freudenstein parameters of the same linkages, however the symmetry is not present in this representation as the Freudenstein parameter space. Moreover the intersection of the design parameter spaces of planar and spherical 4R linkages is not directly observable in that work.

(a) Twelve lines common to the spherical and planar 4R design parameter spaces.
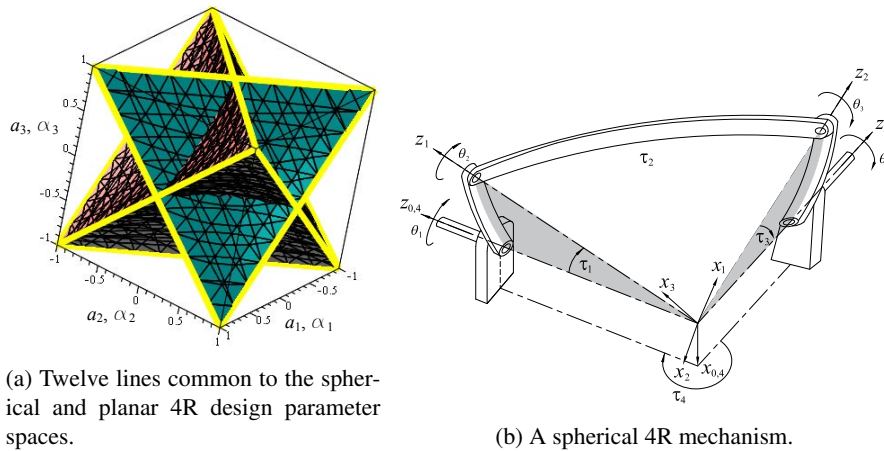
(b) A spherical 4R mechanism.

Fig. 2. Design parameter space intersections and a planar RRRP linkage.

In this paper, attention is focused on the design parameter space of the planar RRRP mechanism since no information on this space exists in the literature in the algebraic form of [4, 5]. The algebraic IO equation for planar 4R linkages is collected in terms of the variable input link angle parameter, $v_1 = \tan(\theta_1/2)$, and the variable slider translation, a_3. The result is a 4th order planar curve in v_1 and a_3 with algebraic properties very different from that of the planar 4R. These properties and their implications will be discussed. The algebraic IO equation of the RRRP linkage contains only four bilinear factors in the design constants a_1, a_2, and a_4. Treating these three a_i as mutually orthogonal basis directions reveals the structure of the four planes that the four bilinear factors imply. Moreover, the mobility conditions on the input joint range of angular displacement implied by the location of a point in this space will be derived.

2. PLANAR RRRP ALGEBRAIC IO EQUATION

Consider the planar RRRP linkage illustrated in Fig. 3a. The variables are the input joint angle θ_1' and the slider translation distance a_3' while the design parameters are the constant link lengths a_1, a_2, a_4', and the inclination angle of the P-pair, $v_4' = \tan(\theta_4'/2)$. Re-collecting Eq. (1) in terms of $v_1' = \tan(\theta_1'/2)$ and a_3' yields an IO equation. Without loss in generality, the general design constant slider angle θ_4', illustrated in Fig. 3a, can always be set to $\pi/2$ with a suitable transformation of the x_0'-y_0' coordinate system, such that the distance a_4' along the x_0'-axis is transformed to the different distance a_4 along the new x_0-axis which is

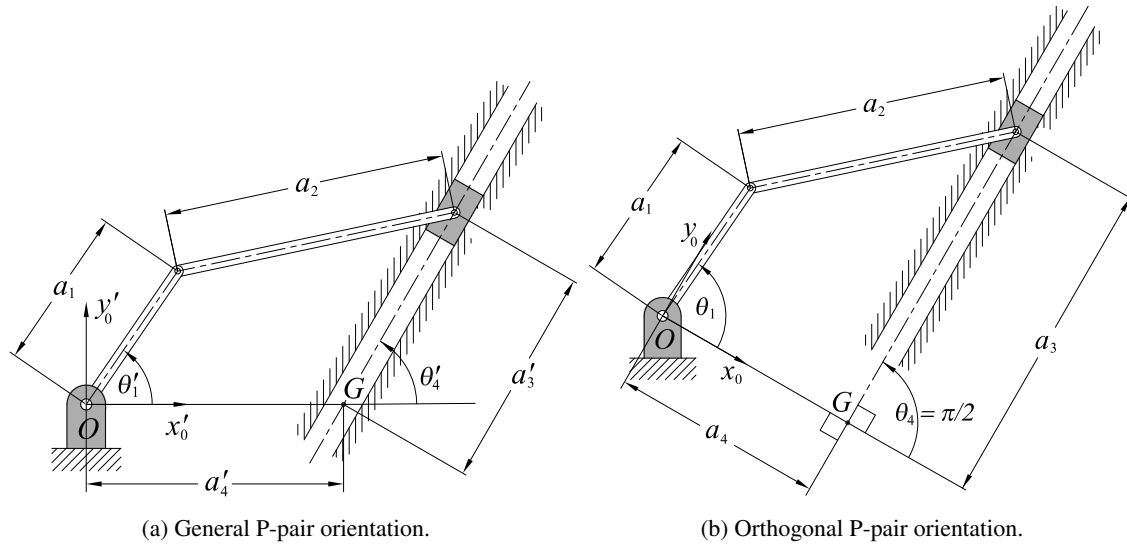(a) General P-pair orientation. (b) Orthogonal P-pair orientation.

Fig. 3. Planar RRRP linkage.

orthogonal to the longitudinal axis of symmetry (the centre-line) of the slider, as illustrated in Fig. 3b. This will change the length of a'_4 to a generally different a_4 and the location of point G on the P-pair longitudinal centre-line thereby changing the zero for the slider translation a_3. Regardless, any RRRP linkage can be so represented [10, 11]. Making the substitution in the IO equation makes several terms vanish revealing a more compact and elegant, but still completely general, RRRP algebraic IO equation:

$$v_1^2 a_3^2 + A v_1^2 + a_3^2 - 4 a_1 v_1 a_3 + B = 0, \tag{2}$$

where

$$
\begin{aligned}
A &= (a_1 + a_2 + a_4)(a_1 - a_2 + a_4) = A_1 A_2, \\
B &= (a_1 + a_2 - a_4)(a_1 - a_2 - a_4) = B_1 B_2, \\
v_1 &= \tan\left(\frac{\theta_1}{2}\right); \quad v_4 = \tan\left(\frac{\theta_4}{2}\right) = \tan\left(\frac{\pi/2}{2}\right) = 1.
\end{aligned}
$$

3. INTERPRETING THE PLANAR RRRP ALGEBRAIC IO EQUATION

Analysing Eq. (2) using the theory of planar algebraic curves [10, 12] one can easily prove that the general algebraic IO equation for planar RRRP linkages has the following three characteristics which are independent of the three constant design parameter lengths a_1, a_2, a_4, and constant angle parameter v_4 [3].

1. Eq. (2) is of degree $n = 4$ in variables v_1 and a_3 and is therefore a quartic curve in the plane spanned by v_1 and a_3. The shape characteristics of individual IO curves are determined by the link lengths a_1, a_2, and a_4.

2. The homogeneous form of this quartic curve, Eq. (3), contains two double points each located at the intersections with the line at infinity of the v_1- and a_3-axes in the v_1-a_3 plane.

$$k_h := v_1^2 a_3^2 + A v_1^2 w^2 + a_3^2 w^2 - 4 a_1 v_1 a_3 w^2 + B w^4 = 0. \tag{3}$$

3. The quartic IO curve can have either genus $g = 1$ or $g = 0$. Therefore, the maximum number of assembly modes of the associated linkage becomes $m = g + 1$ [13, 14], which is 2 for IO curves of

genus 1. It will be shown that IO equations for folding RRRP mechanisms possess genus 0, while all other non-folding planar RRRP mechanisms have quartic IO curves that are genus 1.

3.1. Transition Linkages

A folding RRRP mechanism has link lengths that allow it to fold when $v_1 = 0$ and $a_3 = 0$ making a_1 and a_2 align with a_4 on the x_0-axis. There are only two ways in which the values of a_1, a_2, a_4 lead to an IO curve with a third real finite double point and genus $g = 0$. Each requires that both $v_1 = 0$ and $a_3 = 0$ simultaneously, and that coefficient $B = 0$. Since there are no real values of the link lengths that lead to both $B_1 = 0$ and $B_2 = 0$ simultaneously, then either $a_2 = a_1 + a_4$ or $a_2 = a_1 - a_4$. These are the exact conditions required for an RRRP linkage that can fold with links a_1, a_2, and of course a_4, all aligned on the x_0-axis. Such linkages are called transition linkages since they only have one assembly mode, but two distinct ranges of motion. The input link is a crank, but the output link is restricted to two ranges: $a_3 \geq 0$ or $a_3 \leq 0$. In the folded configuration $a_3 = 0$ implying that the mechanism can transition between either range of motion.
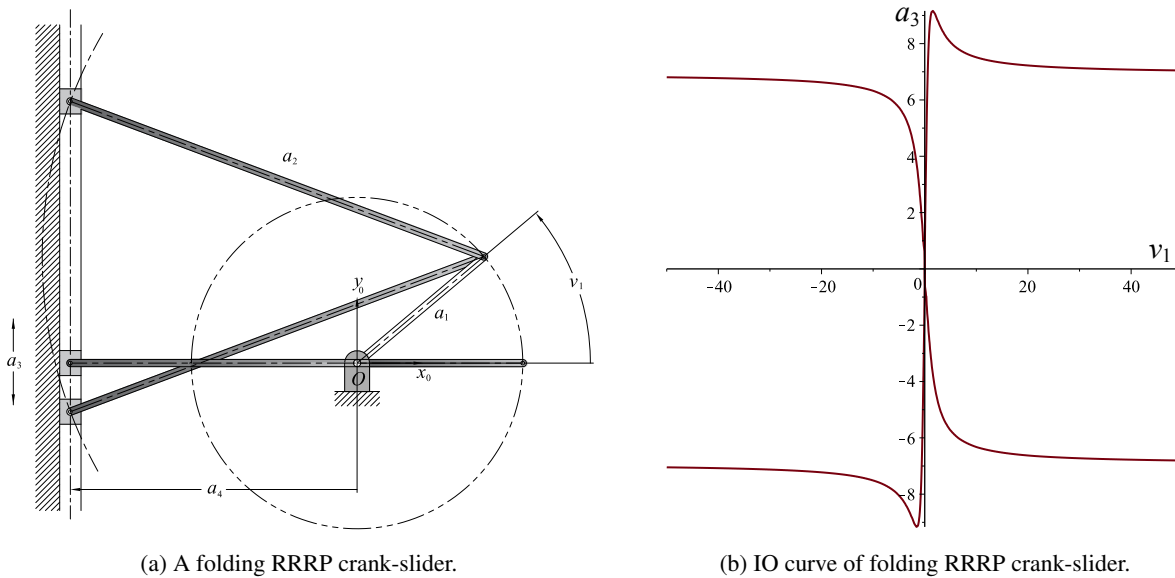

(a) A folding RRRP crank-slider.

(b) IO curve of folding RRRP crank-slider.

Fig. 4. A folding RRRP transition crank with $a_1 = 3$, $a_2 = 7$, and $a_4 = -4$.

The IO curve for such a transition linkage has the finite double point at the IO curve origin $(v_1, a_3) = (0,0)$, as illustrated in Fig. 4b. The double point can be approached from any branch of the IO curve and may be exited along any one of the four paths as well, nicely illustrating the transition behaviour. For any specified value of v_1 there are two possible values for a_3 and for any desired value of a_3 there are two possible values for v_1 with the exception of the finite double point.

3.2. Negative Link Lengths

The link lengths in any mechanical system can be thought of as directed distances. Suppose that the line containing link a_1 is defined by a unit position vector locating the point $(x, y) = (1, 1)$. Multiplying the vector by the scalar -1 simply rotates the vector direction by $\pi = 180°$ making it locate the point $(x, y) = (-1, -1)$. Both vectors are oriented at $45°$ relative to the positive x-axis and their magnitudes are both $\sqrt{2}$, but they point in opposite directions. For the linkage in Fig. 5, the orientation of a_1 is defined by the angle θ_1, but link a_1 points in the opposite direction if it has a negative directed length.

The sign of the coupler directed distance, a_2, is of no consequence in the shape coefficients of the RRRP algebraic IO equation. Only the coefficients A and B in Eq. (2) contain the coupler length a_2. Expanding
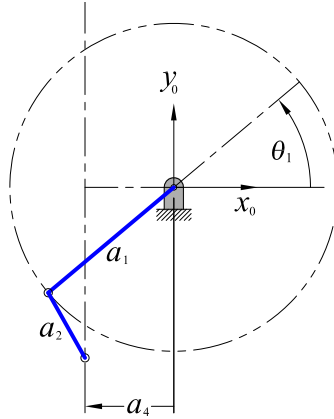
Fig. 5. Negative link length meaning for a_1 and a_4.

these two coefficients leads to

$$A = A_1A_2 = (a_1+a_2+a_4)(a_1-a_2+a_4) = a_1^2+2a_1a_4-a_2^2+a_4^2; \qquad (4)$$
$$B = B_1B_2 = (a_1+a_2-a_4)(a_1-a_2-a_4) = a_1^2-2a_1a_4-a_2^2+a_4^2. \qquad (5)$$

The shape of the algebraic IO equation of every planar RRRP function generating mechanism contains the term $-a_2^2$, which is always a negative number regardless of the sign of the numerical value of a_2. However, the complete mobility classification of the input link requires both positive and negative values of the coupler directed length $\pm a_2$. Since the coupler correlates the rotation of the input link to the translation (linear, or curvilinear) of the slider then directed distance $+a_2$ points from the distal R-pair centre of the input link to the R-pair connecting the coupler to the slider. The directed distance $-a_2$ simply points in the opposite direction: from the R-pair centre connecting the coupler to the slider to the distal R-pair centre of the input link. Therefore, relative to the non-moving coordinate system x_0-y_0, the direction of the length a_2 has no effect on the generated function, but it's sign affects the input link mobility classification.

Whereas, the factors A and B both contain the term $2a_1a_4$, so the signs of the numerical values of the parameters a_1 and a_4 must be considered. Since a_4 always points along the x_0-axis, a negative value for this distance simply places the slider centre line along the negative x_0-axis.

3.3. Assembly Modes and Working Modes

The algebraic IO curve is of degree four and can have multiple closed branches and self-intersects. If the IO curve has two distinct branches, then in order for the linkage to cover points in both branches it must be taken apart and reassembled in a different way. These two distinct linkage configurations, one for each branch of the curve, are called *assembly modes*.

Working modes are subtly different. When the input angle reaches minimum or maximum values the mechanism instantaneously stops moving as the coupler becomes horizontal. In these configurations the mechanism is said to be *locked* because the coupler force line of action is perpendicular to the slider travel direction. A torsional spring in the R-pair connecting the coupler to the slider, or some other form of force capacitance, must be designed into the joint to make the slider move again, thereby breaking the lock. In Fig. 6a the two assembly modes each have two working modes. The two working modes in each assembly mode are separated by the minimum and maximum input angle parameters which occur at the two vertical tangent points on each IO curve branch and represent $v_{1_{min}}$ and $v_{1_{max}}$ in the v_1-a_3 plane. At all other points on the IO curve a vertical line intersects it in an upper value for a_3 and a lower value.

(a) Rocker: $a_1 = 6$, $a_2 = 1$, $a_4 = 2$.

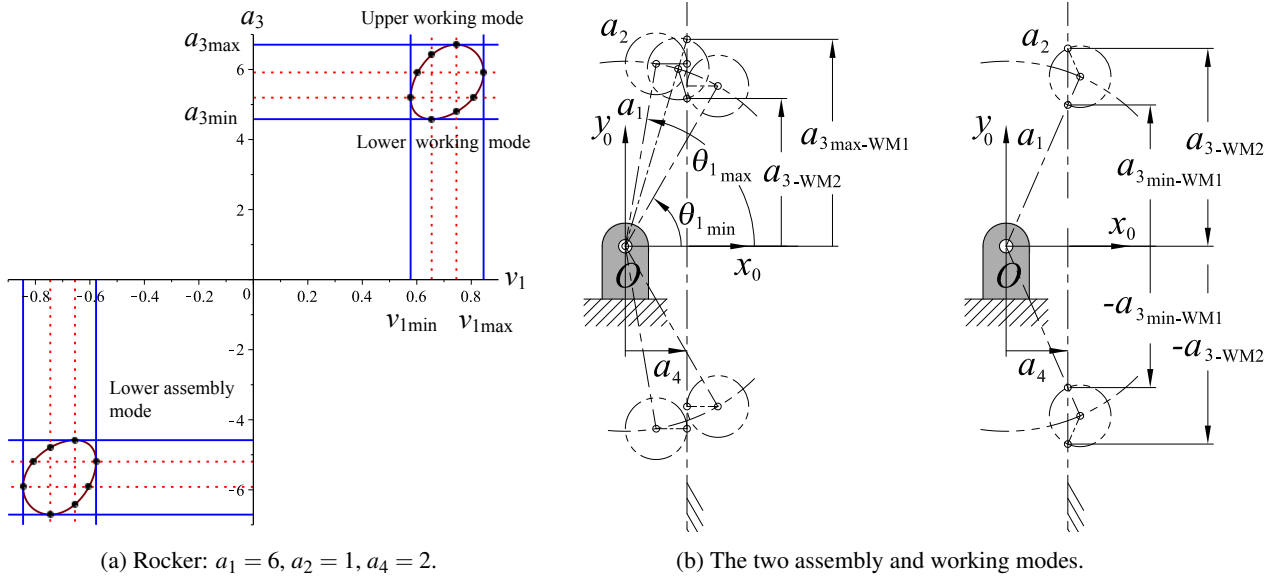(b) The two assembly and working modes.

Fig. 6. Assembly and working modes for an RRRP.

Assembly modes correspond to distinct branches of the IO curve in the v_1-a_3 plane. Working modes are similarly easily identified: if a vertical line parallel to the a_3-axis intersects a distinct branch of the IO curve in two points then there are two working modes in that assembly mode.

Input link	Assembly modes	Working modes
Crank	2	1 in each assembly mode
Rocker	2	2 in each assembly mode
π-rocker	1	2
0-rocker	1	2

Table 1. Assembly and working modes.

4. COMPUTING EXTREMA USING DIFFERENTIAL CALCULUS: SINGULARITY ANALYSIS

4.1. Computing $v_{1_{\text{crit}}}$ to Determine $a_{3_{\text{min/max}}}$: Input Singularity

To determine $a_{3_{\text{min/max}}}$ we must first determine the critical values of v_1 which will be labelled as $v_{1_{\text{crit}}}$, which also determine *input singularities* [15]. Solving the RRRP algebraic IO equation for a_3 yields two solutions, which are the two working modes within each assembly mode:

$$a_3 = \frac{(2a_1v_1) \pm \sqrt{-\left((a_1 - a_2 + a_4)v_1^2 - a_1 - a_2 + a_4\right)\left((a_1 + a_2 + a_4)v_1^2 - a_1 + a_2 + a_4\right)}}{v_1^2 + 1}. \quad (6)$$

Now our algebraic IO equation is expressed as $a_3 = f(v_1)$. The minimum and maximum values for a_3 are obtained by computing the critical values $v_{1_{\text{crit}}}$ of Equation (6). These critical values, if they exist, cause the derivative of a_3 with respect to v_1 to vanish.

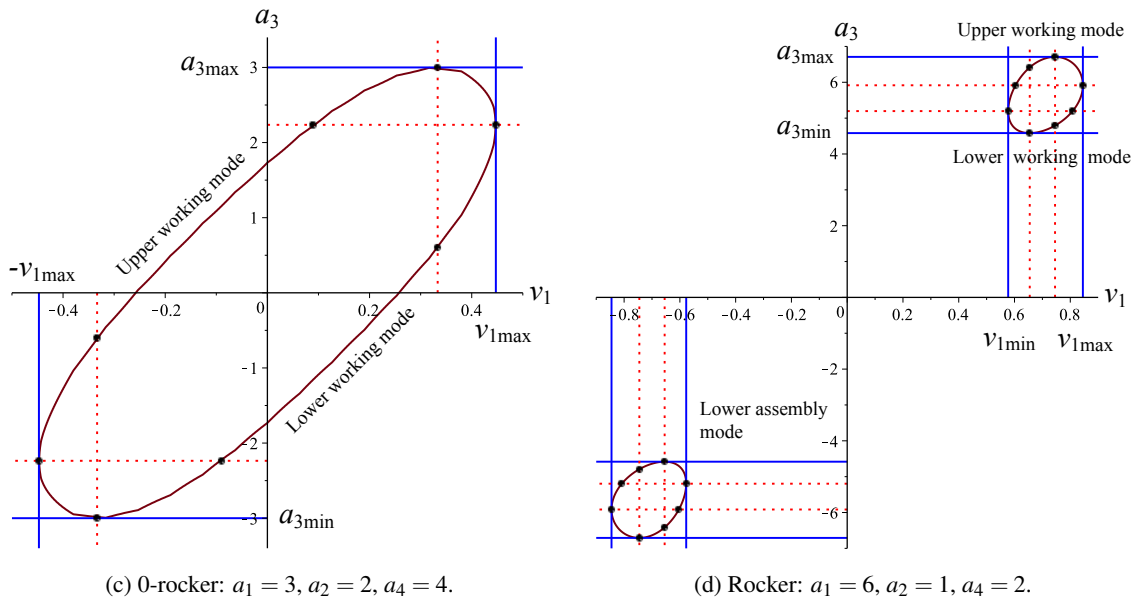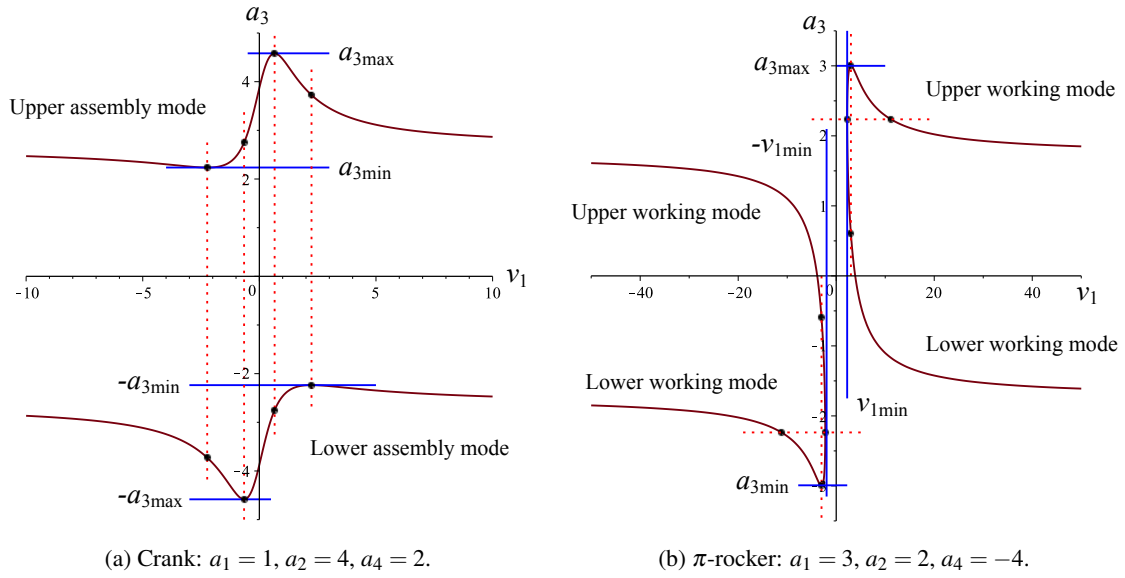$$\frac{\partial a_3}{\partial v_1} = 0. \quad (7)$$

(a) Crank: $a_1 = 1$, $a_2 = 4$, $a_4 = 2$.

(b) π-rocker: $a_1 = 3$, $a_2 = 2$, $a_4 = -4$.

(c) 0-rocker: $a_1 = 3$, $a_2 = 2$, $a_4 = 4$.

(d) Rocker: $a_1 = 6$, $a_2 = 1$, $a_4 = 2$.

Fig. 7. IO curves in the v_1-a_3 coordinate plane.

$$v_{1_{crit_1}} = \pm\frac{\sqrt{(a_1 + a_2 + a_4)(a_1 + a_2 - a_4)}}{a_1 + a_2 + a_4} = \pm\frac{\sqrt{A_1 B_1}}{A_1}; \tag{8}$$

$$v_{1_{crit_2}} = \pm\frac{\sqrt{(a_1 - a_2 + a_4)(a_1 - a_2 - a_4)}}{a_1 - a_2 + a_4} = \pm\frac{\sqrt{A_2 B_2}}{A_2}. \tag{9}$$

Because the double point at infinity on the a_3-axis in the v_1-a_3 plane is isolated (an acnode) then at least one of the critical values of v_1 from Eq. (8) or Eq. (9) must always exist. In other words, $v_{1_{crit_1}}$ and $v_{1_{crit_2}}$

	Input link	$v_{1_{\text{crit}_1}} = \pm\frac{\sqrt{A_1 B_1}}{A_1}$	$v_{1_{\text{crit}_2}} = \pm\frac{\sqrt{A_2 B_2}}{A_2}$	$a_{3_{\text{crit}_1}} = \pm\sqrt{A_1 B_2}$	$a_{3_{\text{crit}_2}} = \pm\sqrt{A_2 B_1}$	Angle limit
1.	Crank	$\mathbb{R}$	$\mathbb{R}$	$\mathbb{C}$	$\mathbb{C}$	None
2.	NA	$\mathbb{C}$	$\mathbb{R}$	$\mathbb{C}$	$\mathbb{C}$	NA
3.	NA	$\mathbb{R}$	$\mathbb{C}$	$\mathbb{C}$	$\mathbb{C}$	NA
4.	NA	$\mathbb{C}$	$\mathbb{C}$	$\mathbb{C}$	$\mathbb{C}$	NA
5.	Rocker	$\mathbb{R}$	$\mathbb{R}$	$\mathbb{R}$	$\mathbb{R}$	$\pm\theta_{1_{\text{min/max}}}$
6.	NA	$\mathbb{C}$	$\mathbb{R}$	$\mathbb{R}$	$\mathbb{R}$	NA
7.	NA	$\mathbb{R}$	$\mathbb{C}$	$\mathbb{R}$	$\mathbb{R}$	NA
8.	NA	$\mathbb{C}$	$\mathbb{C}$	$\mathbb{R}$	$\mathbb{R}$	NA
9.	NA	$\mathbb{R}$	$\mathbb{C}$	$\mathbb{R}$	$\mathbb{R}$	NA
10.	NA	$\mathbb{R}$	$\mathbb{C}$	$\mathbb{C}$	$\mathbb{C}$	NA
11.	NA	$\mathbb{C}$	$\mathbb{R}$	$\mathbb{R}$	$\mathbb{R}$	NA
12.	NA	$\mathbb{C}$	$\mathbb{R}$	$\mathbb{C}$	$\mathbb{C}$	NA
13.	π-rocker	$\mathbb{R}$	$\mathbb{C}$	$\mathbb{R}$	$\mathbb{C}$	$\pm\theta_{1_{\text{min}}}$
14.	0-rocker	$\mathbb{R}$	$\mathbb{C}$	$\mathbb{C}$	$\mathbb{R}$	$\pm\theta_{1_{\text{max}}}$
15.	0-rocker	$\mathbb{C}$	$\mathbb{R}$	$\mathbb{R}$	$\mathbb{C}$	$\pm\theta_{1_{\text{max}}}$
16.	π-rocker	$\mathbb{C}$	$\mathbb{R}$	$\mathbb{C}$	$\mathbb{R}$	$\pm\theta_{1_{\text{min}}}$

Table 2. Complete input link mobility classification: $\mathbb{R}$ = real number; $\mathbb{C}$ = complex number; NA = not assemblable.

cannot simultaneously be complex. Depending on the signed link lengths $\pm a_1$, $\pm a_2$, and $\pm a_4$, it can be shown that the radicands of $\sqrt{A_1 B_1}$ and $\sqrt{A_2 B_2}$ cannot simultaneously be complex.

4.2. Computing $a_{3_{\text{crit}}}$ to Determine $v_{1_{\text{min/max}}}$: Output Singularity

The classification scheme for the angular displacement limits of the input link a_1 depends on the critical values of a_3, abstractly labelled as $a_{3_{\text{crit}}}$, which also determine *output singularities* [15]. If the algebraic IO curve possesses no vertical tangents then input link joint angle limits do not exist. To identify the critical values of a_3 we must first solve the RRRP algebraic IO equation for v_1, rearranging the algebraic IO equation as the function $v_1 = f(a_3)$. There are two solutions, which represent the two possible assembly modes of the mechanism:

$$v_1 = \frac{(2a_1 a_3) \pm \sqrt{-(a_1^2 + a_2^2 - a_3^2 - a_4^2 + 2a_1 a_2)(a_1^2 + a_2^2 - a_3^2 - a_4^2 - 2a_1 a_2)}}{a_1^2 + 2a_1 a_4 - a_2^2 + a_3^2 + a_4^2}. \tag{10}$$

We now equate the partial derivative of v_1 with respect to a_3 to zero. If the critical values of a_3 exist then the angular displacement limits of the input link are computed as $v_{1_{\text{min/max}}} = f(a_{3_{\text{crit}}})$. It is to be seen that the existence of $a_{3_{\text{crit}}}$ requires either, or both, of Eqs. (12) and (13) to be real valued.

$$\frac{\partial v_1}{\partial a_3} = 0. \tag{11}$$

$$a_{3_{\text{crit}_1}} = \pm\sqrt{(a_1 + a_2 + a_4)(a_1 - a_2 - a_4)} = \pm\sqrt{A_1 B_2}; \tag{12}$$

$$a_{3_{\text{crit}_2}} = \pm\sqrt{(a_1 - a_2 + a_4)(a_1 + a_2 - a_4)} = \pm\sqrt{A_2 B_1}. \tag{13}$$

The observations based on the results of numerous examples are listed in Tab. 2. Negative values for directed link lengths a_1 and a_4 have been considered.

5. PLANAR RRRP DESIGN PARAMETER SPACE

In the context of the parametrisation used to obtain Eq. (2) the four bilinear coefficient factors A_1, A_2, B_1, and B_2 each contain one of the four possible permutations of addition to, and subtraction from, a_1 of the remaining link lengths a_2 and a_4. These bilinear factors can be thought of as four distinct planes in a space spanned by three mutually orthogonal basis direction vectors for each one of the link lengths a_1, a_2, and a_4, which we call the *design parameter space*. Each distinct point in the space represents the three directed link lengths of a distinct planar RRRP linkage. These four planes each contain a triangular face of a regular square pyramid whose axis is perpendicular to the plane $a_4 = 0$, illustrated in Fig. 8c. The four planes bound four distinct regions in planes parallel to $a_4 = 0$, where each bounded region contains points representing linkages with different input link mobility characteristics. We will consider intersections of a_1 and a_2 with planes where a_4 is greater than, less than, and identically equal to zero. Different non-zero values for a_4 simply scale the amplitude of a desired slider position as a function of the input angle parameter: $a_3 = a_4 f(v_1)$. Fig. 8c shows intersections of the design parameter pyramid with the three planes $a_4 = \pm 1$ and $a_4 = 3$, illustrating the scaling effect for different values of a_4. Fig. 8a illustrates the intersection of the regular square pyramid with the plane $a_4 = 1$ while Fig. 8b illustrates the intersection of the regular square pyramid with the plane $a_4 = -1$.

In each intersection of a_1 and a_2 with planes where $a_4 > 0$ the four parameter planes of the algebraic IO equation, Eq. (2) intersect each plane $a_4 < 0$ in the four plane traces illustrated in Fig. 8a. These traces have the equations $A_1 = 0$, $A_2 = 0$, $B_1 = 0$, and $B_2 = 0$. Linkages consisting of points on these plane traces represent either folding linkages or non-movable structures. Points in the regions separated by the plane traces represent linkages with very specific displacement capabilities, while points on the interior of the square that has vertices $(a_1, a_2) = (\pm 1, 0)$, $(0, \pm 1)$ represent non-assemblable linkages. We will now determine which linkage types occupy the eight distinct trace-bound regions on the exterior of the unit squares illustrated in Fig. 9.

(a) Intersection with the plane $a_4 = 1$.   (b) Intersection with the plane $a_4 = -1$.   (c) Pyramid-plane intersections.
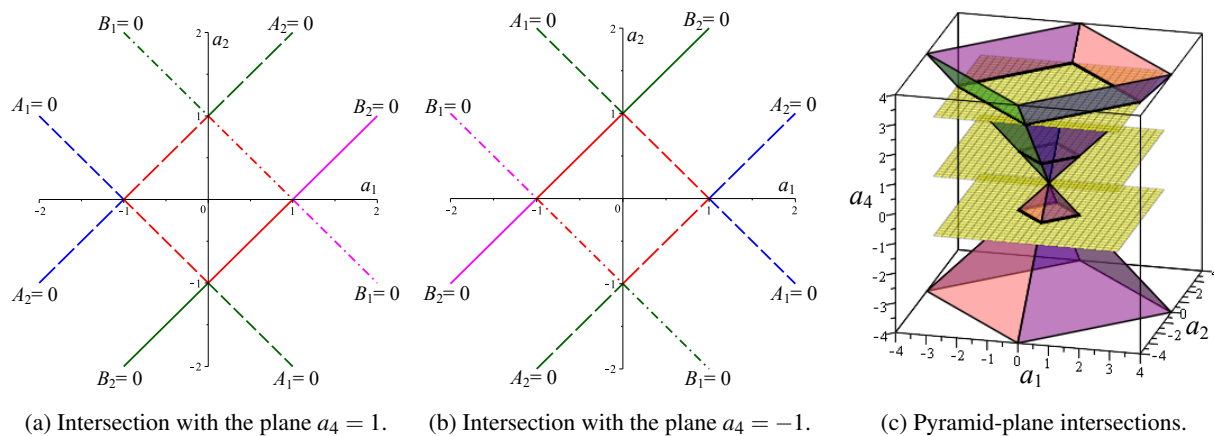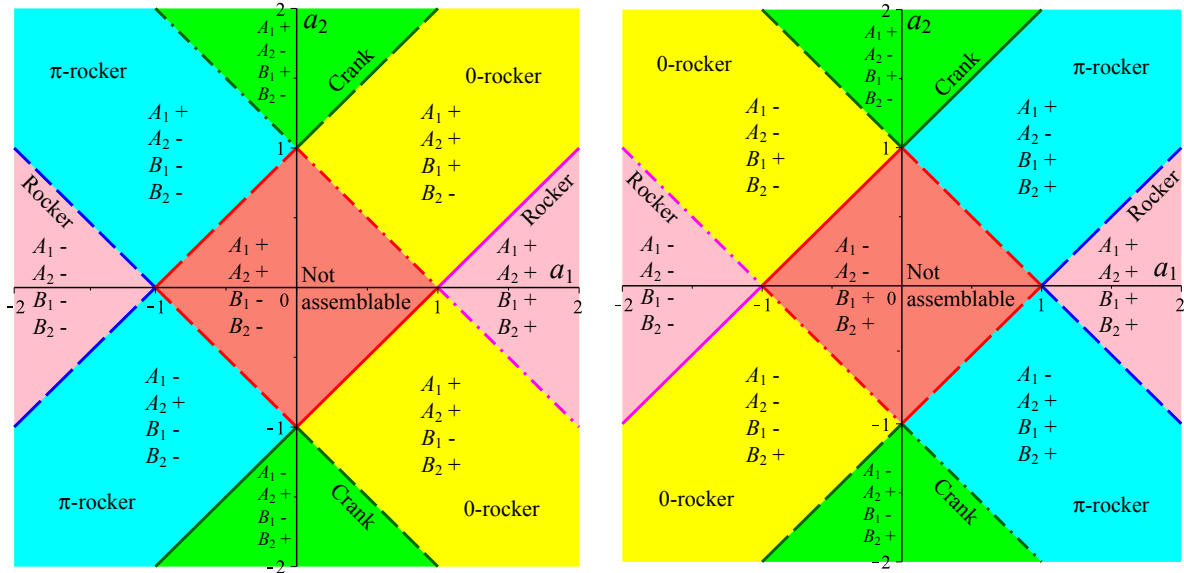
Fig. 8. RRRP design parameter space.

(a) Linkage type regions in the plane $a_4 = 1$.

(b) Linkage type regions in the plane $a_4 = -1$.

Fig. 9. Feasible linkage type regions within the design parameter space in the planes $a_4 = \pm 1$.

5.1. Design Parameter Subspaces for RRRP Linkages

The traces of the plane faces of the design parameter pyramid in the two families of planes where $a_4 > 0$ and $a_4 < 0$, as well as the plane $a_4 = 0$, beg at least three questions.

Question 1. What is the significance of the points of intersection of the four plane traces, i.e. the vertices $(a_1, a_2) = (\pm 1, 0)$, $(0, \pm 1)$ of the square, or any location on the a_1- and a_2-axes?

The answer this first question is relatively straightforward. Four different pairs of plane traces intersect in four different points on the a_1- and a_2-axes at the four different coordinates $(\pm 1, 0)$ and $(0, \pm 1)$. Each point requires either a_1 or a_2 to have zero length. The resulting linkage has no mobility because it consists of two R-pairs having the same axis, and the third connected to the slider. Such a linkage is a rigid structure with zero mobility, if it can be assembled at all. The same holds true for any point located on either of the a_1- or a_2-axes.

Question 2. What is the significance of the location of a point within the nine distinct regions bounded by the four traces?

To answer this question we now consider all distinct permutations of complex and real values for the critical numbers, first discussed in Section 4 where four permutations were demonstrated. However, there are 16 possible permutations of the four critical numbers with two potential outcomes, real or complex. The permutations are listed in Tab. 2, which gives us the classification scheme for the existence of input angle limits. This differential algebraic classification is completely general, free from trigonometric relations, and accounts for all possibilities of positive and negative directed link lengths. Moreover, once the critical values have been computed, it is remarkably straight forward to classify the mobility of the input link using the observations described in [3, 16–18].

Consider the planes $a_4 > 0$, one of which is illustrated in Figs. 8a and 9a. We can immediately observe that the input link mobility is symmetric with respect to the a_1-axis, indicating that the sign of the numerical value of a_2 is irrelevant for the shape coefficients of the IO equation, only its absolute value plays a role. That is, the sign of the length of the coupler is not required to determine the algebraic IO equation. However,
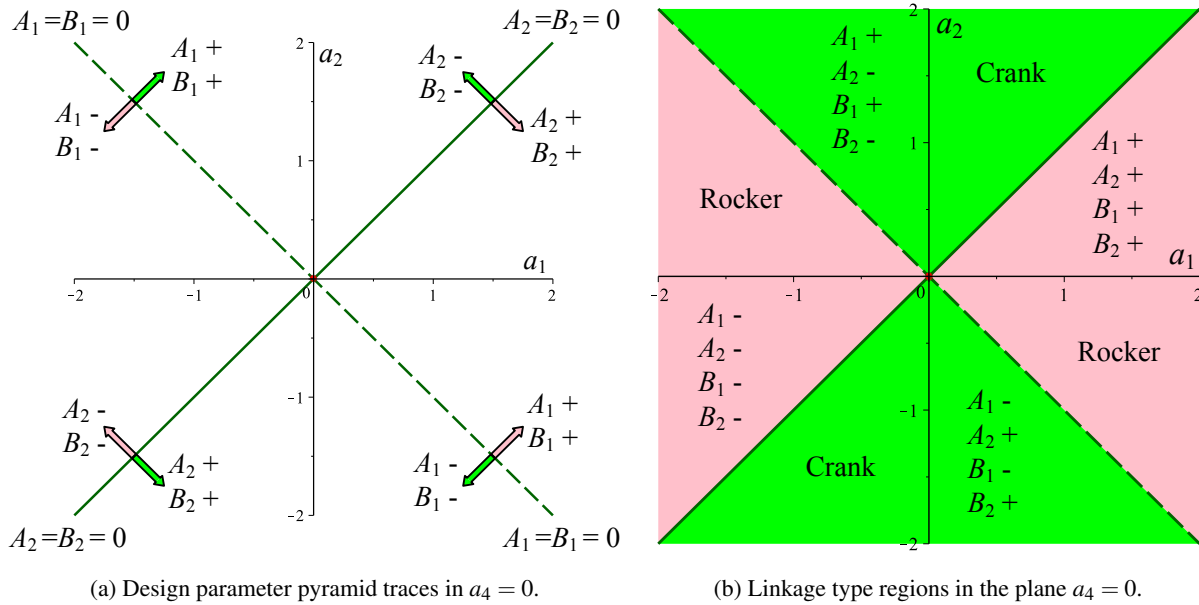
(a) Design parameter pyramid traces in $a_4 = 0$.

(b) Linkage type regions in the plane $a_4 = 0$.

Fig. 10. RRRP design parameter space in the plane $a_4 = 0$.

examining Fig. 9, the signs of a_1, a_2, and a_4 are all required for determining mobility limits of the input link.

Question 3. What is the significance of points laying on the plane traces themselves?

In regions where the associated linkages can be assembled, they can be foldable cranks, foldable 0-rockers or foldable π-rockers. Recall that the definition of a folding RRRP linkage is that links a_1, a_2, and a_4 can align along the x_0-axis necessitating the $a_3 = 0$ while simultaneously $\theta_1 = 0$, or π, in turn meaning that the half-angle input parameter $v_1 = 0$, or ∞. Hence, by their very definition, planar RRRP linkages whose input links are rockers can never fold, because they are restricted to rock in the range between $\theta_{1_{min}}$- $\theta_{1_{max}}$ where $\theta_{1_{min}} \geq 0$ and $\theta_{1_{max}} \leq \pi$ above the x_0-axis, or below the x_0-axis in the range between $-\theta_{1_{min}} \leq 0$ and $-\theta_{1_{max}} \geq \pi$. Folding linkages correspond to points laying on the boundary border-lines in Figs. 9 and 10.

6. CONCLUSIONS

In this paper we have investigated the design parameter space for planar RRRP mechanisms. Using the general RRRP algebraic IO equation, factors of link lengths are identified that define a regular square pyramid in the parameter space of the three directed link lengths a_1, a_2, and a_4, with a_3 being the P-pair excursion parameter. Locations of unique points in that space define unique planar RRRP mechanisms with input and output mobility limits implied by the location of the individual points. These results provide a comprehensive numerical classification scheme based on algebraic parameters, but it also provides an elegant and straight forward graphical method to design planar RRRP linkages with desired mobility characteristics.

Planar RRRP function generating linkages with positive slider offset distances, $a_4 > 0$, zero offset, $a_4 = 0$, and negative offset distances, $a_4 < 0$ are all conveniently represented in three plane intersections $a_4 = 1$, $a_4 = 0$, and $a_4 = -1$. Since these function generators are all conveniently scaled by non-zero values for the offset, without loss in generality, all planar RRRP function generators with desired input link motion characteristics can be both synthesised and analysed using Figs. 9 and 10. Note that these results free the planar RRRP synthesis and analysis tasks from the representational complications imposed by trigonometry and the ultimately non-linear Freudenstein design parameters.

7. ACKNOWLEDGEMENTS

REFERENCES

1. Hartenberg, R. and Denavit, J. *Kinematic Synthesis of Linkages*. McGraw-Hill, Book Co., New York, N.Y., U.S.A., 1964.
2. Ceccarelli, M. *Distinguished Figures in Mechanism and Machine Science, Their Contributions and Legacies Part 1*. Springer, New York, U.S.A., 2007.
3. Rotzoll, M., Hayes, M.J.D. and Husty, M.L. "An Algebraic Input-Output Equation for Planar RRRP and PRRP Linkages." *Proceedings of the 10th CCToMM Symposium on Mechanisms, Machines, and Mechatronics*, École de technologie supérieure, Montréal, QC, Canada, May 16-17, 2019.
4. Rotzoll, M., Hayes, M.J.D., Husty, M.L. and Pfurner, M. "A General Method for Determining Algebraic Input-output Equations for Planar and Spherical 4R Linkages." pp. 96–97. Advances in Robotic Kinematics 2020, eds. Lenarčič, J. and Parenti-Castelli, V., Springer Nature Switzerland AG, Cham, Switzerlnd, 2020.
5. Hayes, M.J.D., Rotzoll, M., Ingalls, C. and Pfurner, M. "Design Parameter Space of Spherical Four-bar Linkages." pp. 19–27. New Trends in Mechanism and Machine Science, EuCoMeas, eds. Pisla, D., Corves, B., and Vaida, C., Springer Nature Switzerland AG, Cham, Switzerlnd, 2020.
6. Coxeter, H.S.M. *Regular Polytopes, 3rd Edition*. Dover Publications, Inc., New York, N.Y., U.S.A., 1973.
7. McCarthy, J.M. "Planar and Spatial Rigid Motion as Special Cases of Spherical and 3-Spherical Motion." *Journal of Mechanisms, Transmissions, and Automation in Design*, Vol. 105, No. 3, pp. 569–575, 1983.
8. Gosselin, C.M. and Angeles, J. "Mobility Analysis of Planar and Spherical Linkages." *Computers in Mechanical Engineering*, July/August 1988.
9. Gosselin, C.M. and Angeles, J. "Optimization of Planar and Spherical Function Generators as Minimum-defect Linkages." *Mechanism and Machine Theory*, Vol. 24, No. 4, pp. 293–307, 1989.
10. Husty, M., Karger, A., Sachs, H. and Steinhilper, W. *Kinematik und Robotik*. Springer-Verlag, Berlin, Germany, 1997.
11. Hunt, K. *Kinematic Geometry of Mechanisms*. Clarendon Press, Oxford, England, 1978.
12. Primrose, E. *Plane Algebraic Curves*. MacMillan, 1955.
13. Husty, M.L. and Pfurner, M. "An Algebraic Version of the Input-Output Equation of Planar Four-Bar Mechanisms." pp. 746–757. *International Conference on Geometry and Graphics*, Milan, Italy, 2018.
14. Harnack, A. "Über die Vielteiligkeit der ebenen algraischen Kurven." In "Mathematische Annalen," pp. 189–198, 1876.
15. Gosselin, C.M. and Angeles, J. "Singularity Analysis of Closed-loop Kinematic Chains." *IEEE Transactions on Robotics and Automation*, Vol. 6, No. 3, p. 281–290, 1990.
16. Murray, A.P. and Larochelle, P.M. "A Classification Scheme for Planar 4*R*, Spherical 4*R*, and Spatial *RCCR* Linkages to Facilitate Computer Animation." *Proceedings of 1998 ASME Design Engineering Technical Conferences (DETC'98)*, Atlanta, Georgia, U.S.A., September 13-16, 1998.
17. McCarthy, J.M. and Soh, G.S. *Geometric Design of Linkages, 2nd Edition* Interdiciplinaty Applied Mathematics. Springer, New York, N.Y., 2011.
18. Hayes, M.J.D., Rotzoll, M. and Husty, M.L. "Design Parameter Space of Planar Four-bar Linkages." Proceedings of the 15th IFToMM World Congress, June 30-July 4, 2019.